LLNL-PROC-661058

LAWRENCE LIVERMORE NATIONAL LABORATORY

Toward A Fundamental Understanding Of Nuclear Reactions And Exotic Nuclei

S. Quaglioni, G. Hupin, J. Langhammer, C. Romero-Redondo, M. D. Schuster, C. W. Johnson, P. Navratil, R. Roth

September 23, 2014

Advances In Radioactive Isotope Science 2014 (ARIS2014)
Tokyo, Japan
June 1, 2014 through June 6, 2014

LLNL-PROC-661058

Toward a Fundamental Understanding of Nuclear Reactions and Exotic Nuclei

Sofia QUAGLIONI[1], Guillaume HUPIN[1], Joachim LANGHAMMER[2], Carolina ROMERO-REDONDO[1], Micah D. SCHUSTER[3], Calvin W. JOHNSON[3], Petr NAVRÁTIL[4], Robert ROTH[2]

[1]*Lawrence Livermore National Laboratory, P.O. Box 808, L-414, Livermore, California 94551, USA*
[4]*Institut für Kernphysik, Technische Universität Darmstadt, D-64289 Darmstadt, Germany*
[3]*San Diego State University, 5500 Campanile Drive, San Diego, California 92182, USA*
[2]*TRIUMF, 4004 Wesbrook Mall, Vancouver, British Columbia, V6T 2A3, Canada*

E-mail: quaglioni1@llnl.gov

(Received Sep 23, 2014)

Nuclear systems near the drip lines offer an exciting opportunity to advance our understanding of the interactions among nucleons, which has so far been mostly based on the study of stable nuclei. However, this is not a goal devoid of challenges. From a theoretical standpoint, it requires the capability to address within an *ab initio* framework not only bound, but also resonant and scattering states, all of which can be strongly coupled. In recent years, significant progress has been made in *ab initio* nuclear structure and reaction calculations based on input from Quantum Chromodynamics employing Hamiltonians constructed within chiral effective field theory. In this contribution, we present a brief overview of one of such methods, the *ab initio* no-core shell model with continuum, and its applications to nucleon and deuterium scattering on light nuclei. The first investigation of the low-lying continuum spectrum of ^{6}He within an *ab initio* framework that encompasses the ^{4}He+n+n three-cluster dynamics characterizing its lowest particle-decay channel will also be briefly presented.

KEYWORDS: *ab initio* calculations, exotic nuclei, low-energy reactions

1. *Ab initio* nuclear theory including the continuum

Light exotic nuclei offer an exciting opportunity to test our understanding of nuclear properties in terms of forces emerging from the underlying theory of Quantum Chromodynamics (QCD). This is not a goal devoid of challenges. Experimentally, the study of rare nuclei is challenged by their short half lives and minute production cross sections. A major stumbling block in nuclear theory has to deal with the low breakup thresholds, which can lead to multi-particle emissions, and can cause bound, resonant and scattering states to be strongly coupled. Even worse, many of the systems we are interested in are simply unbound. Hence, to achieve a fundamental understanding of exotic nuclei we need both advanced experimental techniques and an *ab initio* nuclear theory including the continuum. In the following we briefly outline the elements of one of such theories, the *ab initio* no-core shell model with continuum (NCSMC).

1.1 Nuclear forces

To develop such an *ab initio* theory, we start from nuclear interactions grounded in the underlying theory of Quantum Chromodynamics via chiral effective field theory [1–3], where nucleons and pions are the only explicit degrees of freedom and the strong interaction is systematically expanded in terms of positive powers of small momenta Q (the generic momentum in the nuclear process or the pion mass) over the chiral symmetry breaking scale $\Lambda \sim 1$ GeV. The nuclear forces emerging from such a procedure order by order are schematically represented by the diagrams of Fig. 1. In particular, we

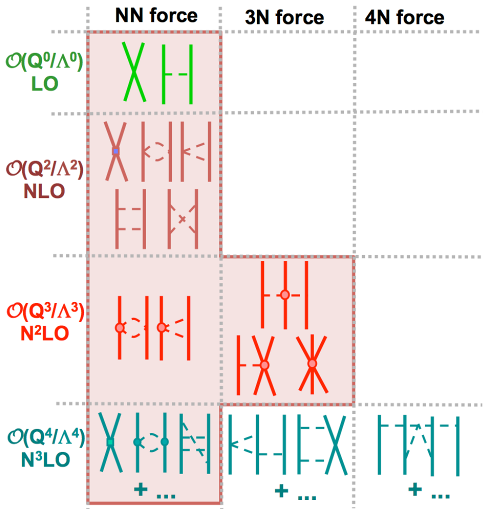

Fig. 1. Schematic of chiral EFT interactions. Solid lines represent nucleons and dashed lines pions. The contour highlights the terms employed in the many-body calculations presented here.

adopt a Hamiltonian based on the chiral N^{3}LO NN interaction of Ref. [4] and N^{2}LO 3N force of Ref. [5]. Except for the ^{9}Be results of Sec. 2.2, these are interactions that are entirely constrained in the two- and three-body [6] systems, and will be used to make predictions for heavier systems.

1.2 Similarity renormalization group method

The next crucial requirement for an *ab initio* theory including the continuum is to achieve converged results working within the large but finite model spaces that are accessible with modern supercomputers. To achieve this, we soften the chiral interactions using the similarity renormalization group (SRG) method [7–10]. This employs a continuous unitary transformation of the Hamiltonian

$$H_\lambda = U_\lambda H_{\lambda=\infty} U_\lambda^\dagger \,, \tag{1}$$

that can be written as a flow equation with respect to a parameter λ with units of momentum,

$$\frac{dH_\lambda}{d\lambda} = -\frac{4}{\lambda^5}[\eta(\lambda), H_\lambda] \,, \tag{2}$$

where $\eta(\lambda)$ is a generator commonly chosen to be the commutator of the evolved Hamiltonian with the kinetic energy operator, $\eta(\lambda) = [T, H_\lambda]$. As λ evolves from infinity (corresponding to the bare Hamiltonian) towards zero, low- and high-momentum parts of the interaction become more and more decoupled so that convergence of many-body calculations can be reached working in increasingly smaller model spaces, as shown in Fig. 2(a) for the ground-state (g.s.) energy of the ^{4}He nucleus. Here bare and SRG-evolved $NN + 3N$ interactions converge to the same final result for the energy. Only the convergence rate is much faster with the SRG interactions. A drawback of this method (as for other modern effective interactions) is that the evolution induces three- and higher-body (up to A-body) terms into the Hamiltonian, even when starting from a bare NN interaction. Fortunately, for $A \leq 12$ stopping at three-body terms leads to energies [10] and phase shifts [11] mostly independent of λ, i.e. the unitarity of the transformation is preserved. In addition, when using SRG-evolved Hamiltonians, for consistency one should also evolve any other operator using the same unitary transformation [12, 13]. As an example, Fig. 2(b) shows the effect of induced two-and three-body terms for the expectation value of the evolved r^2 operator on the ^{3}H g.s. wave function. The unitarity of the transformation is fully recovered once all terms up to the three-body level are included.

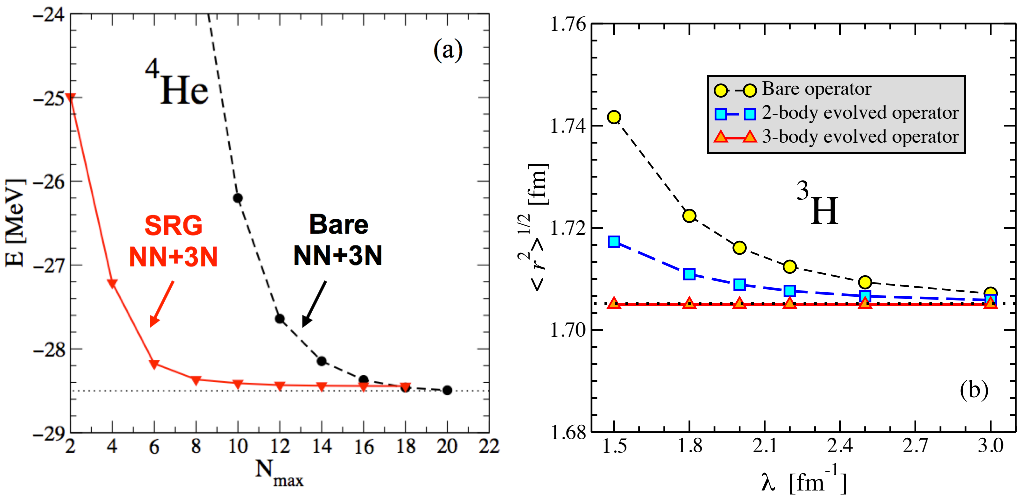

Fig. 2. The (a) g.s. energy of the ^{4}He nucleus as a function of the NCSM model-space size $N_{\max}$ and (b) root-mean-square matter radius of tritium as a function of the SRG momentum scale λ. In panel (a), results obtained with the bare chiral $NN + 3N$ forces (dashed line) are compared with those obtained after SRG evolution to $\lambda = 2.0$ fm^{-1} (solid line). In panel (b), lines with circles, squares and triangles correspond to calculations with the SRG-evolved $NN + 3N$ Hamiltonian and bare, 2-body evolved and 3-body evolved operators, respectively. In both panels, the thin dotted lines show the converged bare result.

1.3 No-core shell model with continuum

The *ab initio* no-core shell model with continuum [14, 15] provides a unified framework for the description of structural and reaction properties of light nuclei. In this approach the nuclear many-body states are seen as superimpositions of square-integrable energy eigenstates of the A-nucleon system, $|A\alpha J^\pi T\rangle$, and continuous resonating-group method (RGM) [16, 17] wave functions,

$$|\Phi^{J^\pi T}_{\nu r}\rangle = \Big[\Big(|A-a\ \alpha_1 I_1^{\pi_1} T_1\rangle |a\ \alpha_2 I_2^{\pi_2} T_2\rangle\Big)^{(sT)} Y_\ell(\hat{r}_{A-a,a})\Big]^{(J^\pi T)} \frac{\delta(r-r_{A-a,a})}{r r_{A-a,a}} \,. \tag{3}$$

Here, a target and a projectile composed of $A-a$ and $a \le A$ nucleons, respectively and whose centers of mass are separated by the relative coordinate $\vec{r}_{A-a,a}$ are traveling in a $^{2s}\ell_J$ wave of relative motion (with s the channel spin, and ℓ the relative momentum of the system). The index $\nu = \{A-a\,\alpha_1 I_1^{\pi_1} T_1;\ a\,\alpha_2 I_2^{\pi_2} T_2;\ s\ell\}$ collects all quantum numbers associated with this continuous basis . For each channel of total angular momentum, parity and isospin ($J^\pi T$), the resulting NCSMC translational-invariant ansatz is given by:

$$|\Psi^{J^\pi T}_A\rangle = \sum_\alpha c^{J^\pi T}_\alpha |A\alpha J^\pi T\rangle + \sum_\nu \int dr\, r^2 \frac{\gamma^{J^\pi T}_\nu(r)}{r} \mathcal{A}_\nu |\Phi^{J^\pi T}_{\nu r}\rangle \,. \tag{4}$$

The eigenstates of each cluster of nucleons and of the compound nucleus, identified respectively by the energy labels $\alpha_{1(2)}$ and α, are antisymmetric under exchange of internal nucleons. They are consistently obtained ahead of time by means of the *ab initio* no-core shell model (NCSM) [18] through the diagonalization of their respective microscopic Hamiltonians in finite bases constructed from many-body harmonic oscillator (HO) wave functions with up to $N_{\max}$ HO excitations above the unperturbed configuration and frequency $\hbar\Omega$. The full antisymmetrization of the basis (3) is enforced by introducing an appropriate inter-cluster antisymmetrizer $\mathcal{A}_\nu$. Finally, $c^{J^\pi T}_\alpha$ and $\gamma^{J^\pi T}_\nu(r) = (\mathcal{N}^{-1/2}\chi)_\nu(r)$ are

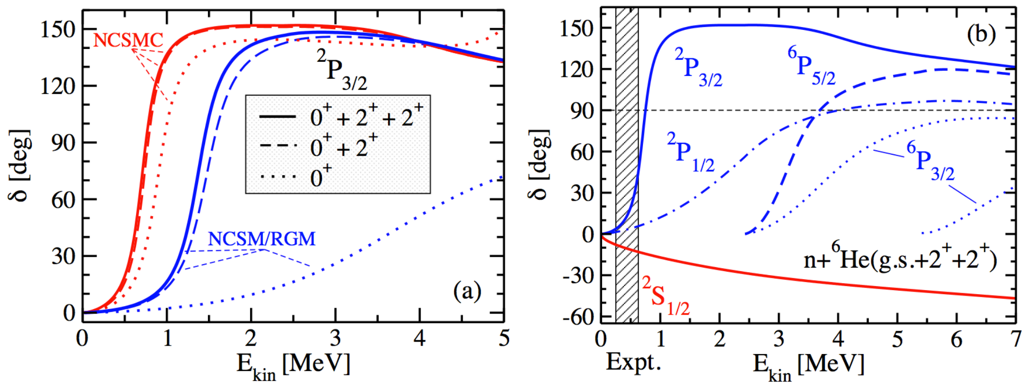

Fig. 3. Diagonal ^{6}He+n phase shifts obtained with the chiral NN potential SRG-evolved to $\lambda = 2.02$ fm^{-1} by working within an $N_{\rm max} = 12$ and $\hbar\Omega = 16$ MeV HO model space. Panel (a) compares NCSM/RGM (blue lines) and NCSMC (red lines) results including the ^{6}He 0^+ g.s. only (dotted lines), 0^+ and 2^+_1 states (dashed lines), and 0^+, 2^+_1 and 2^+_2 states (solid lines). Panel (b) shows S- and P-wave phase shifts calculated with the NCSMC by including the three lowest ^{6}He states. The dashed vertical area indicates the experimental centroid and width of the ^{7}He ground state.

respectively discrete and continuous variational amplitudes, solutions of the coupled equations

$$\begin{pmatrix} E_\alpha\,\delta_{\alpha\alpha'} & (h\mathcal{N}^{-\frac12})_{\alpha\nu'}(r') \\ (h\mathcal{N}^{-\frac12})_{\alpha'\nu}(r) & (\mathcal{N}^{-\frac12}\mathcal{H}\mathcal{N}^{-\frac12})_{\nu\nu'}(r,r') \end{pmatrix}\begin{pmatrix} c_{\alpha'} \\ \frac{\chi_{\nu'}(r')}{r'} \end{pmatrix} = E\begin{pmatrix} \delta_{\alpha\alpha'} & (g\mathcal{N}^{-\frac12})_{\alpha\nu'}(r') \\ (g\mathcal{N}^{-\frac12})_{\alpha'\nu}(r) & \frac{\delta_{\nu\nu'}\delta(r-r')}{rr'} \end{pmatrix}\begin{pmatrix} c_{\alpha'} \\ \frac{\chi_{\nu'}(r')}{r'} \end{pmatrix}. \tag{5}$$

Here, E denotes the total energy of the system and the two by two block-matrices on the left- and right-hand side of the equation represent, respectively, the NCSMC Hamiltonian and norm (or overlap) kernels. In the upper diagonal blocks are the Hamiltonian (overlap) matrix elements over the discrete A-nucleon states. Similarly, those over the orthonormalized continuous portion of the basis appear in the lower diagonal block and are obtained from $\mathcal{N}_{\nu\nu'}(r,r') = \langle\Phi^{J^\pi T}_{\nu r}|\mathcal{A}_\nu\mathcal{A}_{\nu'}|\Phi^{J^\pi T}_{\nu' r'}\rangle$ and $\mathcal{H}_{\nu\nu'}(r,r') = \langle\Phi^{J^\pi T}_{\nu r}|\mathcal{A}_\nu H\mathcal{A}_{\nu'}|\Phi^{J^\pi T}_{\nu' r'}\rangle$. The off diagonal blocks contain the couplings between the two sectors of the basis, with $g_{\alpha\nu}(r) = \langle A\,\alpha J^\pi T|\mathcal{A}_\nu|\Phi^{J^\pi T}_{\nu r}\rangle$ and $h_{\alpha\nu}(r) = \langle A\,\lambda J^\pi T|H\mathcal{A}_\nu|\Phi^{J^\pi T}_{\nu r}\rangle$. The scattering matrix (and from it any scattering observable) follows from matching the solutions of Eq. (5) with the known asymptotic behavior of the wave function at large distances by means of the microscopic R-matrix method [19, 20]. Finally we note that, in principle, the expansion of Eq. (4) can be further generalized to include a three-cluster component suitable for the description of, e.g., Borromean halo nuclei and reactions with final three-body states [21, 22].

2. Applications

2.1 The unbound ^{7}He nucleus as a testing ground

An ideal system to showcase new achievements made possible by the *ab initio* NCSMC is ^{7}He [14]. The unified description of the structural and reaction properties of this unbound nucleus cannot be realized within the traditional NCSM. One could calculate its properties within a ^{6}He+n binary-cluster expansion, that is by retaining only the second term of Eq. (4) and solving $\mathcal{N}^{-\frac12}\mathcal{H}\mathcal{N}^{-\frac12}\chi = E\chi$. The results of such an approach, which we call NCSM/RGM [23], are indicated by the blue lines in Fig. 3(a). However, ^{6}He is a loosely bound nucleus, so its polarization plays an important role, as can be seen from the dependence of the NCSM/RGM results on the number of six-body cluster eigenstates included in the calculation. Further, a limitation (due to computational limitations) to just

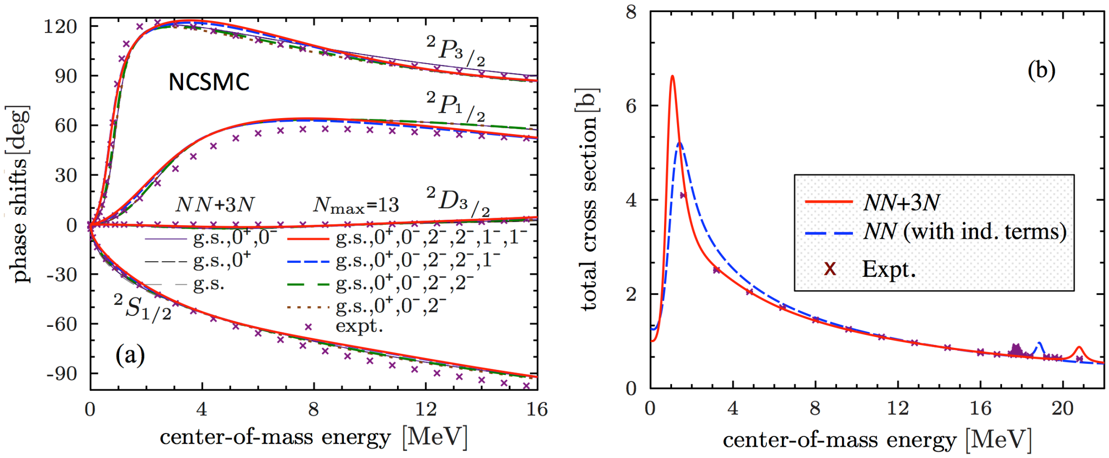

Fig. 4. Computed (lines) ^{4}He+n (a) phase shifts and (b) total cross section obtained with the chiral $NN + 3N$ Hamiltonian SRG-evolved to $\lambda = 2.0$ fm^{-1} by working within the NCSMC at $N_{\text{max}} = 13$ and $\hbar\Omega = 20$ MeV compared to experiment (crosses). Panel (a) shows the convergence with respect to the inclusion of the first seven low-lying states of the ^{4}He target (indicated in the legend). In panel (b) the effect of the initial chiral $3N$ force is highlighted by comparing the full result (red solid line) with that obtained with the chiral NN interaction SRG-evolved at the three-body level (dashed blue line).

a few of the lowest ^{6}He eigenstates in the NCSM/RGM expansion would be questionable especially because, except for the lowest 2^+ state, all other ^{6}He excited states are either broad resonances or simply states in the continuum. With the NCSMC these challenges are overcome. As shown by the red lines in Fig. 3(a), the further inclusion of square integrable energy-eigenstates of the ^{7}He nucleus (in the present calculation four $3/2^-$ states, of which only the first produces a substantial effect on the $^2P_{3/2}$ resonance) compensates for missing higher ^{6}He excitations, leading to a much faster convergence rate. Finally, the present NCSMC calculation yields the well established $3/2^-$ g.s. and $5/2^-$ resonances close to measurements, but does not support the presence of a narrow low-lying $1/2^-$ state advocated by some [24]. Instead, the $^2P_{1/2}$ results of Fig. 3(b) are in fair agreement with the $1/2^-$ properties measured in the neutron pick-up and proton-removal experiments of Ref. [25].

2.2 Three-nucleon forces and continuum

One of the questions we are trying to answer by means of *ab initio* calculations is what is the role of the chiral $3N$ force in scattering observables and in the (near) continuum spectrum of light nuclei. The unbound ^{5}He nucleus is an excellent testing ground for such an endeavor. Earlier studies of its g.s. and $1/2^-$ resonances have demonstrated that they are sensitive to the strength of the spin-orbit component of the nuclear Hamiltonian, part of which is carried by the $3N$ force [23, 26]. A NCSM/RGM investigation of the elastic scattering of nucleons on ^{4}He using for the first time the chiral $NN + 3N$ Hamiltonian was recently published in Ref. [11]. However, significant variations of the $^2P_{3/2}$ and $^2P_{1/2}$ phase shifts at low-energy as a function of the number of states (the first seven) used to describe the ^{4}He nucleus did not allow for definitive conclusions on the ability of the present Hamiltonian to reproduce the observed ^{5}He properties. As shown in Fig. 4(a), this issue can be solved by carrying out NCSMC calculations, where the model space of Ref. [11] is augmented by coupling fourteen (of which three $3/2^-$ and one $1/2^-$) NCSM eigenstates of the ^{5}He compound nucleus [15]. As for the ^{7}He nucleus in the previous section, the convergence with respect to the number of target states is now excellent. Further, the total cross section, presented in Fig. 4(b), reproduces the experimental data rather well and the $3N$ force plays a fundamental role in reaching such an agreement.

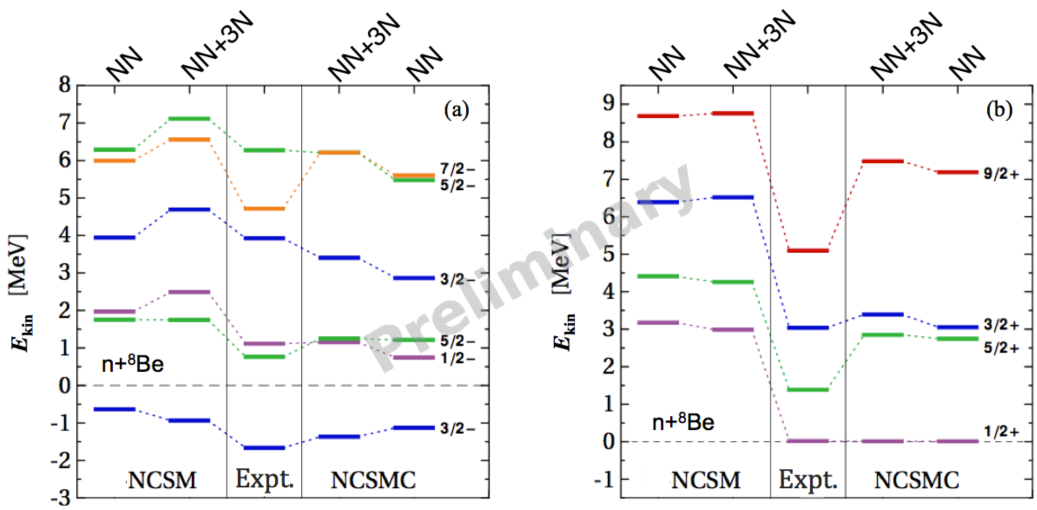

Fig. 5. Computed low-lying energy spectrum of ^{9}Be (a) negative- and (b) positive-parity states compared to experiment. The chiral $NN + 3N$ Hamiltonian of Ref. [29] with evolution parameter $\lambda = 2$ fm^{-1} was used. The negative(positive)-parity NCSMC calculation, coupling ^{9}Be square integrable eigenstates with ^{8}Be$(0^+, 2^+)$ binary cluster states, was performed in a $N_{\rm max} = 12(11)$, $\hbar\Omega = 20$ MeV HO model space. Here $E_{\rm kin}$ indicates the center-of-mass energy with respect to the ^{8}Be+n threshold.

To further investigate the interplay between $3N$-force and continuum effects, we carried out NCSMC calculations with the chiral $NN + 3N$ interactions for the structure of ^{9}Be. This is a notoriously challenging-to-describe nucleus for *ab initio* approaches based on bound-state techniques such as the NCSM. The positive parity resonances are in general found too high compared to experiment and the splitting between the lowest $5/2^-$ and $1/2^-$ resonances [highlighted in Fig.5(a)] tends to be overestimated when $3N$ effects are included [27]. Here we discuss preliminary results obtained by studying ^{9}Be as a linear combination of 9-body square-integrable eigenstates and ^{8}Be+n binary-cluster states with the ^{8}Be in its ground and 2^+ state [28]. The splitting between the $5/2^-$ and $1/2^-$ levels is substantially reduced when the continuum is included due to a shift towards lower energies of the $^2P_{1/2}$ resonance. However, the most dramatic continuum effects are found in the positive-parity resonances, shown in Fig. 5(b). The $1/2^+$ and the $3/2^+$ S-wave resonances are several MeV lower in the NCSMC, close to their experimental value.

A similar investigation was also performed for the ^{6}Li nucleus. While lighter than ^{9}Be, the computational challenge in describing this nucleus comes from its low-lying ^{4}He+d particle-emission threshold. Building upon the NCSM/RGM framework of Ref. [30], the NCSMC formalism to treat deuterium-nucleus scattering was recently developed and first applied to describe this system using chiral $NN + 3N$ interactions [31]. Figure 6 shows preliminary results for the ^{6}Li energy spectrum of states and their widths, obtained in a $N_{\rm max} = 11$ model space containing six-body eigenstates coupled to ^{4}He(g.s.)+d binary cluster wave functions with up to seven deuterium pseudo-excited states in the $^3S_1 - ^3D_1$, $^3D_2$ and $^3D_3 - ^3G_3$ channels. The ^{4}He+d continuum plays an especially important role for the higher-lying 2^+ and 1^+ resonances. Combined with the inclusion of the $3N$ force, the NCSMC yields a rather good agreement with the observed spectrum. Interestingly, the 3^+ excitation energy with respect to the g.s. is not very sensitive to either continuum or $3N$-force effects.

2.3 *Ab initio description of three-cluster dynamics*

Achieving an *ab initio* treatment of the interactions among three nuclear fragments, such as those occurring in Borromean halos or in three-body breakup processes, is another important stepping

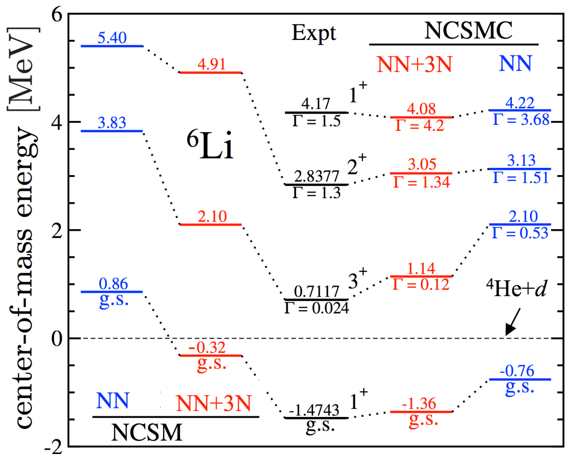

Fig. 6. Computed low-lying spectrum of positive-parity states (and their widths Γ) for the ^{6}Li nucleus with (red lines) and without (blue lines) inclusion of the initial chiral 3N force compared to experiment (black lines). Both NN and NN + 3N Hamiltonians were SRG-evolved at the three-body level, using λ = 2.0 fm^{-1}. Two sets of $N_{\max}$ = 11, $\hbar\Omega$ = 20 MeV results are shown: NCSM calculations of ^{6}Li energy eigenstates, and NCSMC calculations further including ^{4}He+d binary cluster states.

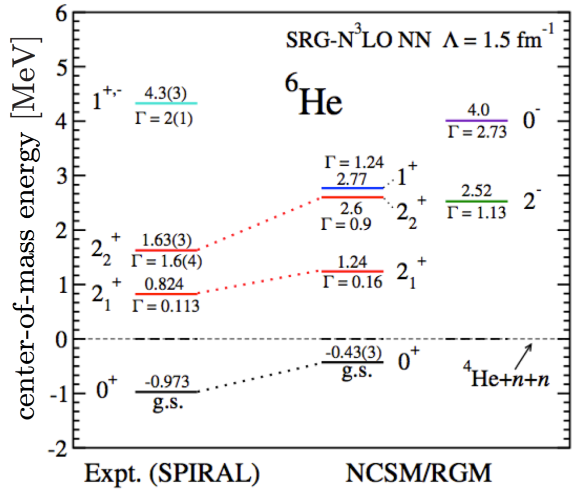

Fig. 7. Positions and widths (indicated by Γ) in MeV of low-lying positive- and negative-parity resonances of the ^{6}He nucleus as obtained from *ab initio* NCSM/RGM calculations of the ^{4}He+n+n scattering phase shifts using the SRG-evolved chiral NN interaction with λ = 1.5 fm^{-1} and an $N_{\max}$ = 13, $\hbar\Omega$ = 14 MeV HO model space compared to new SPIRAL measurements [32] performed at GANIL, France. The figure is taken from Ref. [22].

stone towards gaining a basic understanding of nuclei and their reactions. At present we are in the process of generalizing the NCSMC framework of Sec. 1.3 to include three-cluster basis states. The development of the NCSM/RGM component of the formalism for the treatment of core+n+n systems starting from a two-nucleon Hamiltonian has been completed and recently applied to the description of bound [21] and continuum states [22] of the ^{6}He nucleus within a ^{4}He(g.s.)+n+n cluster basis. The energy spectrum of states obtained with the SRG-evolved chiral NN potential with λ = 1.5 fm^{-1} is shown in Figure 7. We find the known $J^\pi = 2^+$ resonance as well as results consistent with two new resonances recently observedat the SPIRAL facility of Ganil [32]: a second 2$^+$ and a 1$^+$ (the parity of the 4.3 MeV J = 1 state was not determined in the experiment). Additional resonant states, not observed, emerged in the 0$^-$ and 2$^-$ negative-parity channels. At the same time, our three-body scattering phase shifts in the 1$^-$ channel present only a very broad structure and do not support the presence of a low-lying soft dipole mode.

3. Conclusions

The *ab initio* description of light dripline nuclei with QCD-guided NN + 3N forces is now becoming possible, thanks in part to the NCSMC approach. This is an *ab initio* theory including the continuum which combines the efficient description of short- and medium-range correlations of the NCSM with the ability of the NCSM/RGM of describing the scattering physics of a system. This theory is undergoing exciting developments, among which in this contribution we discussed the inclusion of the 3N force in the description of nucleon- and deuteron-nucleus collisions as well as the extension to the treatment of three-cluster dynamics. This is leading us to better understand the interplay between 3N-force and continuum effects in p-shell nuclei such as ^{6}Li and ^{9}Be and to refine our theoretical description of Borromean nuclei such as ^{6}He.

Acknowledgments

Prepared in part by LLNL under Contract DE-AC52-07NA27344. This material is based upon work supported by the U.S. Department of Energy, Office of Science, Office of Nuclear Physics, under Work Proposal Number SCW1158 as well as under Award Numbers DE-FG02-96ER40985 and DE-FC02-07ER41457, the NSERC Grant Number 401945-2011, the Computational Science Research Center at San Diego State University, the Deutsche Forschungsgemeinschaft through Contract SFB 634, the Helmholtz International Center for FAIR within the framework of the LOEWE program launched by the State of Hesse, and the BMBF through Contract No. 06DA7074I. TRIUMF receives funding via a contribution through the Canadian National Research Council. Computing support for this work came from the LLNL institutional Computing Grand Challenge program, the National Energy Research Scientific Computing Center (edison) supported by the Office of Science of the U.S. Department of Energy under Contract No. DE-AC02-05CH11231, the LOEWE-CSC Frankfurt, the computing center of the TU Darmstadt (lichtenberg), and from an INCITE Award on the Titan supercomputer of the Oak Ridge Leadership Computing Facility (OLCF) at ORNL.

References

[1] E. Epelbaum, H.-W. Hammer, and U.-G. Meißner: Rev. Mod. Phys. **81** (2009) 1773.
[2] R. Machleidt and D. R. Entem: Phys. Rep. **503** (2011) 1.
[3] E. Epelbaum and U.-G. Meißner: Annu. Rev. Nucl. Part. Sci. **62** (2012) 159.
[4] D. R. Entem and R. Machleidt: Phys. Rev. C **68** (2003) 041001.
[5] P. Navrátil: Few-Body Syst. **41** (2007) 117.
[6] D. Gazit, S. Quaglioni, and P. Navrátil: Phys. Rev. Lett. **103** (2009) 102502.
[7] S. Głazek and K. Wilson: Phys. Rev. D **48** (1993) 5863; F. Wegner: Ann. Phys. **506** (1994) 77.
[8] S. K. Bogner, R. J. Furnstahl, and R. J. Perry: Phys. Rev. C **75** (2007) 061001.
[9] H. Hergert and R. Roth: Phys. Rev. C **75** (2007) 051001.
[10] E. D. Jurgenson, P. Navrátil, and R. J. Furnstahl: Phys. Rev. Lett. **103** (2009) 082501; Phys. Rev. C **83** (2011) 034301.
[11] G. Hupin, J. Langhammer, P. Navrátil, S. Quaglioni, A. Calci, and R. Roth: Phys. Rev. C **88** (2013) 054622.
[12] E. R. Anderson, S. K. Bogner, R. J. Furnstahl, and R. J. Perry: Phys. Rev. C **82** (2010) 054001.
[13] M. D. Schuster, S. Quaglioni, C. W. Johnson, E. D. Jurgenson, and P. Navrátil: Phys. Rev. C **90** (2014) 011301.
[14] S. Baroni, P. Navrátil, and S. Quaglioni: Phys. Rev. Lett. **110** (2013) 022505; Phys. Rev. C **87** (2013) 034326.
[15] G. Hupin, S. Quaglioni, and P. Navrátil: arXiv:1409.0892v1 (2014).
[16] Y. Tang, M. LeMere, and D. Thompsom: Physics Reports **47** (1978) 167.
[17] K. Langanke and H. Friedrich: *Advances in Nuclear Physics* (Plenum, New York, 1987) Chapter 4.
[18] P. Navrátil, J. P. Vary, and B. R. Barrett: Phys. Rev. Lett. **84** (2000) 5728; Phys. Rev. C **62** (2000) 054311.
[19] M. Hesse, J.-M. Sparenberg, F. Van Raemdonck, and D. Baye: Nucl. Phys. A **640** (1998) 37.
[20] M. Hesse, J. Roland, and D. Baye: Nucl. Phys. A **709** (2002) 184.
[21] S. Quaglioni, C. Romero-Redondo, and P. Navrátil: Phys. Rev. C **88** (2013) 034320.
[22] C. Romero-Redondo, S. Quaglioni, P. Navrátil, and G. Hupin: Phys. Rev. Lett. **113** (2014) 032503.
[23] S. Quaglioni and P. Navrátil: Phys. Rev. Lett. **101** (2008) 092501; Phys. Rev. C **79** (2009) 044606.
[24] K. Markenroth, *et al.*: Nucl. Phys. A **679** (2001) 462; M. Meister, *et al.*: Phys. Rev. Lett. **88** (2002) 102501; F. Skaza, *et al.*: Phys. Rev. C **73** (2006) 044301; N. Ryezayeva, *et al.*: Phys. Let. B **639** (2006) 623.
[25] A. H. Wuosmaa, *et al.*: Phys. Rev. C **72** (2005) 061301; Phys. Rev. C **78** (2008) 041302.
[26] K. M. Nollett, S. C. Pieper, R. B. Wiringa, J. Carlson, and G. M. Hale: Phys. Rev. Lett. **99** (2007) 022502.
[27] C. Forssén, P. Navrátil, W. E. Ormand, and E. Caurier: Phys. Rev. C **71** (2005) 044312.
[28] J. Langhammer, P. Navrátil, S. Quaglioni, G. Hupin, and R. Roth: in preparation.
[29] R. Roth *et al.*: Phys. Rev. Lett. **109** (2012) 052501.
[30] P. Navrátil and S. Quaglioni: Phys. Rev. C **83** (2011) 044609.
[31] G. Hupin, S. Quaglioni, and P. Navrátil: in preparation.
[32] X. Mougeot, *et al.*: Physics Letters B **718** (2012) 441.